

Supplementary Materials and Methods

Cell lines, culture conditions and chemicals. Unless otherwise indicated, media and supplements for cell culture were purchased from Gibco-Thermo Scientific (Thermo Fisher Scientific Inc., Waltham, MA) and plastic ware from Corning B.V. Life Sciences (Corning, NY) and Thermo Scientific. Human colorectal carcinoma HCT 116 and adenocarcinoma HT-29 cells [from American Type Culture Collection (ATCC), Manassas, VA] were routinely maintained in McCoy's 5A medium supplemented with 10% fetal calf serum (FCS), 10 mM 4-(2-Hydroxyethyl)piperazine-1-ethanesulfonic acid (HEPES) buffer, 100 units/mL penicillin G sodium salt and 100 µg/mL streptomycin sulfate. Human colon adenocarcinoma DLD-1, SW480 and SW620 cells (from ATCC) were routinely maintained in RPMI-1640 medium supplemented with 10% FCS, 10 mM HEPES buffer, 100 units/mL penicillin G sodium salt, 100 µg/mL streptomycin sulfate. Cancer stem cell (CSC) isolation and culture from human colorectal cancer (CRC) patient samples (all obtained in accordance with the standards of the institutional Ethics Committee on human experimentation, authorization no. CE5ISS 09/282) were performed as previously reported[1, 2]. Surgical specimens were washed several times with phosphate buffered saline (PBS) and subjected to mechanical and enzymatic dissociation. Upon centrifugation for 3 minutes (min) at 150 g, the resulting cancer cells were incubated for 30 min at 37°C under shaking in Dulbecco's Modified Eagle Medium (DMEM) medium supplemented with 1.5 mg/mL collagenase type II, 200 units/mL penicillin G sodium salt and 200 µg/mL streptomycin sulfate. Upon filtering through a 70-µm nylon mesh and centrifugation as described above, pellets were resuspended in CSC isolation medium composed by advanced DMEM/F12 medium supplemented with 2 mM L-glutamine, 2% B-27 supplements, 1% N2-supplement, 20 ng/mL human epidermal growth factor (EGF), 10 ng/mL human fibroblast growth factor (FGF2) (basic) (both from PeproTech Inc., London, UK), 10 mM nicotinamide and 1 µM Y-27632 (both from Sigma-Aldrich, St. Louis, MO), and incubated in

standard culture conditions in ultra-low attachment tissue culture flasks. Spheroids (which were evident after 1 to 3 weeks from sample processing) were routinely maintained in CSC culture medium composed by DMEM/F12 medium containing 2 mM L-glutamine, 0.6% glucose, 9.6 mg/mL putrescine, 6.3 ng/mL progesterone, 5.2 ng/mL sodium selenite, 4 mg/mL heparin sodium salt, 100 ng/mL hydrocortisone, 0.025 mg/mL insulin, 0.1 mg/mL apotrasferrin (Euroclone, Pero, Italy) and supplemented with 20 ng/mL human EGF, 10 ng/mL human FGF2, 10 mM nicotinamide (Sigma-Aldrich), and passaged once a week at dilution 1:2 by mechanical (micropipette) or enzymatic [<5 min at 37°C with TripLE™ Select and Accumax (Sigma-Aldrich) (1:1 dilution)] dissociation. CRC-SCs have been validated for their capability to generate neoplasms faithfully recapitulating the phenotypic heterogeneity of the original patient tumor when xenotransplanted into immunocompromised mice[3]. Cells were seeded as single cells onto the appropriate supports (6-, 24- or 96-well plates) 24 h before the beginning of experiments. Selected CRC-SCs belonging to the three categories (#1 and #4 for high; #3 and #6 for medium and #8, #10 and #12 for low sensitive) were employed in most *in vitro* experiments and included in IHC analyses on multiple CRC-SC-derived xenografts. Of these CRC-SCs, 3 (#1, #3 and #8) were also used in *in vivo* experiments. Additional CRC-SCs were included in specific assays depending on cell availability and status, using as main criterion the balance towards the point of sensitivity to LY2606368. All compounds were provided from Selleck Chemicals with the exception of aphidicolin, colchicine, Mps1-IN-3, nocodazole, reversine, thymidine, UCN-01 (all purchased from Sigma-Aldrich), LY2606368 (also known as prexasertib, provided from Eli Lilly, Indianapolis, IN) and PV1019 (obtained from Calbiochem-Merck Millipore, Billerica, MA). Chemicals included in the drug library were resuspended with dimethyl sulfoxide (DMSO; Sigma-Aldrich) at concentration of 10 μM , subdivided into a library of 5 x 96-well microtiter plates (each containing also two series of DMSO controls) and stored at -80°C . The appropriate amount of DMSO was always employed for negative control conditions (*e.g.*, final concentration 0.02%, v:v for the compound screen).

Compound screening and measurement of cell proliferation/viability. To determine the drug concentration required to inhibit cell proliferation by 50% (IC₅₀) or drug-combination efficiency, 6 x 10³ cells seeded in 96-well plates (100 μL of medium/well) via a multichannel pipet (Mettler-Toledo, Columbus, OH) were cultured for 24 h, then left untreated or treated as indicated in Figure Legends. For drug screening, CRC-SCs were seeded onto 96-well plates with an automated dispensing robot (Multidrop 384, Thermo Fisher Scientific). Upon 48 h to 72 h from (co-)treatment, the cell viability/proliferation was determined by luminescence counting of ATP levels in each well using the CellTiter-Glo[®] Luminescent Cell Viability Assay (Promega, Madison, WI) and a multimode reader (DTX-880; Beckman Coulter, Brea, CA) according to the manufacturer's instructions. Triplicate plates for each combination of CRC-SCs and compound library plate tested were generated. Upon treatment for 72 h with the drug library compounds (**Figure S1, Table S2**), the proxy measure of CRC-SC proliferation and viability was obtained by CellTiter-Glo[®] assay (see above). Normalized viability for each drug (VD) was obtained for each plate by referencing luminescence values (LD) to the averaged values of DMSO controls (mLC) using the following formula: $VD = (LD/mLC) * 100$. The z scores (ZD) were obtained for each CRC-SC line by referencing each normalized viability replicate (VD) to the grand mean (Gm) and grand standard deviation (Gsd) of all compounds using the following formula: $ZD = (VD - Gm) / Gsd$. Analysis of drug screening data was performed using the "R" software (R Foundation for Statistical Computing, Vienna, Austria; <http://www.R-project.org/>) and the following packages: 'plyr' for data table handling, 'ggplot2' for generating plots, 'drc' for the curve fitting of DNA damage response inhibitors data and 'gplots' for IC₅₀ clustering.

Deep Sequencing and Whole Exome Sequencing (WES). Targeted deep DNA resequencing was focused on 17 genes known to be frequently mutated in colon cancer and relevant for targeted therapy or prognosis. An amplicon-based custom panel was developed using the Illumina Design-Studio software (Illumina Inc., San Diego, CA). The library for sequencing was prepared with the

Truseq Custom Amplicon Kit (Illumina) following the manufacturer's instructions. Sequencing was performed on a MiSeq instrument and FASTQ files were analyzed with Miseq Reporter software using the Somatic Variant Caller algorithm (all from Illumina). Variant annotation was carried on with the Illumina Variant Studio suite (Illumina). All the variants with Allele Frequency > 10; coverage > 100x; missense damage consequence; dbSNP MAF < 5% were kept. The OncoPrint (**Table 1**) was generated using custom R scripting and the ComplexHeatmaps library available at <https://github.com/jokergoo/ComplexHeatmap>. Whole Exome Sequencing was performed outsourced by BGI corporation (BGI, Shenzhen, China). Target enrichment was performed using in-solution technology NimbleGen SeqCap EZ Library v.3.0 (Roche, Basel, Switzerland) and the resulting target libraries were sequenced by HiSeq2000 sequencing technology (Illumina) as reported in[3].

Clonogenic assay. For assessing their clonogenicity, CRC-SCs left untreated or exposed for 24h to LY2606368 were dissociated as single cells, resuspended in 0.3% agarose (SeaPlaque Agarose; Cambrex, East Rutherford, NJ) and seeded in quadruplicate in 24-well plates at 500 cells/well or 1000 cells/well over a 0.4% agarose bottom layer. Cells were incubated in drug-free culture medium under standard culture condition for up to 15 days. Colonies were then fixed/stained with 0.1% crystal violet and counted under an inverted microscope. To calculate the survival fraction upon treatment, the number of colonies was normalized to the plating efficiency of untreated cells.

In vivo study. Housing and handling of animals was in strict compliance with national Animal Experimentation Guidelines for Laboratory Animal Welfare (D.L.116/92) and in accordance with the Directive EU 63/2010. All the in vivo experimentations are included in an experimental protocol approved by the Institutional Animal Experimentation Committee. Female NOD.Cg-Prkdcscid Il2rgtm1Wjl/SzJ (NSG) mice (The Jackson Laboratory, Bar Harbor, ME) of 4 to 6-week-old with average body weight of ~21 g were employed after an acclimatization period of 14 days.

Feeding and drinking was ad libitum 24 h per day. For xenograft studies CRC-SCs were resuspended in 50% Matrigel Basement Membrane Matrix (BD Biosciences, Franklin Lakes, NJ)/50% growth medium to a final concentration of 5×10^6 cells/mL. Thereafter, 5×10^5 cells were injected subcutaneously in the flank of mice. Tumors were measured twice a week by a caliper and tumor volumes were determined using the formula: $\pi/6 \times d^2 \times D$, where D and d represent the longest tumor measurements diameter and its perpendicular, respectively. When tumors reached a size of approximately 14 mm^3 (usually within 3 to 5 weeks from the inoculum), mice were randomized to control and treatment groups (10 mice/group) and treated subcutaneously with vehicle only (Captisol; CyDex Pharmaceuticals Inc., La Jolla, CA), or with 5 or 10 mg/kg of the mesylate salt formulation of LY2606368, which has comparable *in vitro* activity and increased *in vivo* bioavailability, as reported in Legend of **Figure 1**. For *in vivo* rescue studies, CSC-derived xenografts were harvested from control or LY2606368-treated mice (6 tumors/group), dissociated as single cells and either analyzed for their *in vitro* clonogenicity (by limiting dilution and soft-agar assay) or injected into secondary mice. All animals were left untreated. *In vivo* tumor growth and tumor volumes were measured as reported above. Animals were euthanized according to the national Animal Welfare Guidelines.

Reverse-phase protein array (RPPA) analysis. CRC-SCs or commercial ATCC CRC lines were seeded at a density of 1×10^5 cells/well onto 24-well plates in duplicates. On the following day, cells left untreated or were treated with LY2606368 at appropriate concentrations and, from 1 h, 4 h, 9 h or 24 h to treatment, collected and lysed in a buffer containing T-PER reagent (Thermo Fisher Scientific), 300 mM NaCl (J.T.Baker; Avantor Performance Materials, Center Valley, PA), protease and phosphatase inhibitors cocktails (Sigma-Aldrich). Samples were incubated on ice for 20 min and centrifuged at 10,000 g for 10 min. Thereafter, supernatants were transferred to fresh tubes and total protein concentration was measured with the Bradford reagent method (Coomassie-based protein assay, Thermo Fisher Scientific). Lysates were then diluted for printing in extraction buffer

containing 47.5% T-PER reagent, 50% 2X Sodium dodecyl sulfate (SDS) (Invitrogen-Thermo Fisher Scientific) and 2.5% Tris(2-carboxyethyl)phosphine hydrochloride (TCEP) reagent (Thermo Fisher Scientific) to a final concentration of 0.5 mg/mL. All samples were printed in technical triplicate as neat and 1:4 dilution pairs onto nitrocellulose-coated glass slides (GRACE Bio-Labs Inc., Bend, OR). Reference standard lysates, i.e. HeLa + Pervanadate (Becton, Dickinson and Company, Franklin Lakes, NJ), A431 + EGF (Becton, Dickinson and Company), Jurkat + Etoposide (Cell Signaling Technology, Danvers, MA) and Jurkat + Calyculin A (Cell Signaling Technology), were printed in 10-point decreasing mixtures of treated to untreated samples as procedural controls and as positive controls for antibody staining. Each reference standard curve was printed in technical triplicate at a final concentration of 0.5 mg/mL. Aushon 2470 arrayer equipped with 185 μm pins (Aushon Biosystems, Billerica, MA) was used to print samples/slides according to the manufacturer's instructions. A selected subset of the printed microarray slides were stained with Sypro Ruby Protein Blot Stain (Thermo Fisher Scientific) to estimate sample total protein concentration and the remaining slides were stored under desiccated conditions at -20°C . Immediately before antibody staining, printed slides were treated with 1X Reblot Mild Solution (Chemicon, Temecula, CA) for 15 min, washed 2 x 5 min with PBS and incubated for 2 h in blocking solution containing 2% I-Block (Applied Biosystems, Foster City, CA) and 0.1% Tween-20 in PBS. Immunostaining was carried out using a tyramide-biotin signal amplification kit (DAKO, Carpinteria, CA). Primary antibody binding was detected using a biotinylated goat anti-rabbit IgG H+L (diluted at 1:7500; Vector Laboratories, Burlingame, CA) or rabbit anti-mouse Ig (diluted at 1:10, DAKO) followed by streptavidin-conjugated IRDye[®] 680LT fluorophore (LI-COR Biosciences, Lincoln, NE). Primary antibodies undergo pre- and post-RPPA validation for single band specificity by western-blot using complex cellular lysates. Negative control slides incubated only with secondary antibody were included in each staining run. All Sypro Ruby and immunostained slides were scanned using a Tecan Power Scanner[™] (Tecan Group Ltd, Männedorf,

Switzerland) at 5 μm resolution. Acquired images were analyzed with MicroVigene v5.2 (VigeneTech, Carlisle, MA) for spot detection, local background subtraction, negative control subtraction, replicate averaging and total protein normalization. The “R” software (see above) equipped with packages ‘plyr’, ‘dplyr’, ‘tidyr’, ‘reshape2’, ‘ggplot2’, ‘coin’, ‘ComplexHeatmap’ and ‘gplots’ was used to carry out slide quality control, internal standardization, two-way hierarchical clustering (Euclidean distance and Ward.D2 method), Kruskal-Wallis and Wilcoxon signed rank non-parametric statistical tests (false discovery rate set to 0.05). A detailed list of antibodies used for RPPA, western-blot and immunohistochemical analyses is available in **Table S4**.

Immunoblotting. The detection of protein levels was performed as previously reported [4]. Briefly, cells were harvested, washed with PBS, lysed for 10 min on ice in the same buffer used for RPPA (see above) and then centrifuged for 15 min at 13 000 rpm. Supernatants were collected and total protein concentration was determined by the Bradford reagent method (Thermo Fisher Scientific). Equal amount of proteins (30 μg) were resolved by SDS-polyacrylamide gel electrophoresis (SDS-PAGE) and electro-transferred to a nitrocellulose membrane (Pierce-Thermo Fisher Scientific). Membranes were incubated overnight with the primary antibody of interest and then for 1 h at room temperature with the appropriate horseradish peroxidase-conjugate secondary antibody. Chemiluminescence 16-bit imaging was performed with the Kodak Image Station 4000R (IS4000R) and the Carestream Molecular Imaging Software version 5.0 (Carestream Health Inc., Rochester, NY), or with G:Box Chemi-XX9 and the GeneSys Software v1.5.6 (Synoptics, Cambridge, UK). The following primary antibodies were used: anti-p21 (diluted at 1:1000; #2947), phospho-ATR (S428) (diluted at 1:1000; #2853), phospho-CHK1 (S317) (diluted at 1:1000; #12302), CHK1 (diluted at 1:750; #2345), phospho-CHK2 (T68) (diluted at 1:1000; #2661), CHK2 (diluted at 1:1000; #3440), γH2AX (S139) (diluted at 1:250; #9718) (all from Cell Signaling Technology), phospho-ATM (S1981) (diluted at 1:500; #ab81292), ATM (diluted at 1:500; #ab78) (both from

Abcam, Cambridge, UK), ATR (diluted at 1:250; #sc-515173), (from Santa Cruz Biotechnology Inc., Dallas, TX) and phospho-RPA32 (S4/S8) (diluted at 1:1000; #A300-245A), phospho-RPA32 (S33) (diluted at 1:1000; #A300-246A), RPA32 (diluted at 1:1000; #A303-874A) (from Bethyl Laboratories Inc., Montgomery, TX). Anti- β -Actin (diluted at 1:1000; #4967, Cell Signaling Technology), anti-C23/Nucleolin (diluted at 1:1000; #sc-8031, Santa Cruz Biotechnology) and anti- α/β Tubulin (diluted at 1:1000; #2148, Cell Signaling Technology) antibodies were used to monitor equal loading of lanes. Densitometric analysis of the western blot bands was performed using ImageJ v1.5 software (NIH, Bethesda, MD, USA; <https://imagej.nih.gov/>). Briefly, relative band intensity was expressed as relative optical density calculated by dividing the area of densitometric profiles of each protein analyte (encompassing the phosphorylated and total form) with the respective loading control. As for the quantification of the phospho/total ratio of a specific protein, the levels of the phosphorylated form were normalized to those of the corresponding total content.

RNA interference, lentiviral particles production and transduction. For transient RNA interference, CRC-SCs seeded at low density in the appropriate support were transfected 8h later with an unrelated small interfering (si) RNA (siCTR) or specific siRNAs directed against CHK1 (siCHK1A and siCHK1B) by means of oligofectamine RNAiMAX transfection reagent (Thermo Fisher Scientific) or HiPerFect Transfection Reagent (Qiagen, Hilden, Germany) according to the manufacturer's instructions. The following Custom-designed siRNAs: 5'-GCCGGUAUGCCGGUUAAGUdTdT-3' (siCTR), and 5'-GCGUGCCGUAGACUGUCCAdTdT-3' (siCHK1B) were purchased from Sigma-Aldrich, while the validated Silencer Select siRNAs directed against CHK1 (s502+s503, CHK1A) from Thermo Fisher Scientific.

For stable shRNA or gene expression in CRC-SCs, we employed (1) the following shRNA-expressing lentiviral vector: GIPZ non-silencing lentiviral shRNA Control (#RHS4348), GIPZ CHEK1 shRNA (#RHS4531-EG1111) and GIPZ TP53 shRNA (#RHS4531-EG7157), which were

all provided by GE Dharmacon, Lafayette, CO), and (2) TOP-GFP.mC and FOP-GFP.mC, which were gifts from Ramesh Shivdasani (Addgene plasmid #35491 and #35492, respectively) [5]. Lentiviral particles were obtained by transfecting the HEK-293T packaging cell line using the X-tremeGENE HP DNA Transfection Reagent (Roche, Basel, Switzerland). Upon 48 h and 72 h, lentiviral supernatants were collected and then concentrated using the Lenti-X Concentrator (Takara/Clontech, Mountain View, CA), according to the manufacturer's instructions. Lentiviral particles were then resuspended in PBS, aliquoted and stored at -80°C. For CRC-SC transduction, 30 µl of concentrated lentiviral particles were added to 3×10^5 cells in medium supplemented with 8 µg/mL of polybrene (Sigma-Aldrich). After 24 h from cell transduction, the culture medium was replaced with fresh medium. Thereafter, CRC-SCs were incubated under standard culture conditions for 48 h prior to the administration of 1 or 1.5 µg/mL of puromycin (Sigma-Aldrich) to start transduced cell selection. Puromycin-resistant cells were used or expanded for experimentation, and stored in liquid nitrogen.

Cytofluorometric studies. To assess the impact of LY2606368 on the expression of surface colorectal-CSC markers, 3×10^5 cells seeded in 6-well plates (3 mL of medium/well) were cultured for 24 h, and then left untreated or treated with 100 nM LY2606368. Upon 24 h or 48 h from treatment, cells were resuspended at 8×10^5 /mL, seeded in 96-well plates (100 µL of medium/well) and stained with CD44v6-purified (clone 2F10) or EphrinB2-AF488 (clone 512012) (both from R&D Systems, Minneapolis, CA at 1:20 dilution in CSC culture medium. Samples were incubated in the dark on ice for 30 min and then washed twice with CSC culture medium. Thereafter, cells were co-stained with the appropriate Alexa Fluor® 488 secondary antibody (diluted at 1:500 in CSC culture medium; Thermo Fisher Scientific) on ice for 30 min. Cells were washed twice before the addition of 100 µL CSC culture medium supplemented with 4'-6-diamidino-2-phenylindole (DAPI, 10 mM) (Molecular Probes-Thermo Fisher Scientific). Analysis of cell cycle progression by cytofluorometry was achieved as previously described[6, 7]. For the assessment of cell cycle

profiling, dissociated CRC-SC spheroids or trypsinized ATCC cell lines were collected and, after a washing with PBS, fixed by gentle vortexing in ice-cold 80% (v/v) ethanol (Sigma-Aldrich). Samples were incubated at least 24 h at -20 °C, then washed twice with PBS and stained with 50 µg/mL propidium iodide (PI) (Sigma-Aldrich) in 0.1% (w/v) D-glucose in PBS supplemented with 1 µg/mL (w/v) RNase A (Sigma-Aldrich) for 30 min at 37°C. Cells were then incubated overnight at 4°C upon flow cytometry-mediated analyses. Alternatively, dissociated living cells were co-stained for 30 min at 37°C with 1 µg/mL PI and 10 µg/mL Hoechst 33342 (Molecular Probes-Thermo Fisher Scientific) for detecting plasma membrane permeabilization and monitoring DNA content, respectively. For the simultaneous measurement of DNA content and phospho-histone H3 (pH3) levels, ethanol-fixed samples were permeabilized with 0.25% (v/v) Tween 20 (Sigma-Aldrich) in PBS at 4°C for 15 min and, upon incubation in 3% (w/v) BSA (Sigma-Aldrich) in PBS for 30 min at 4°C (to block unspecific binding), stained with a primary anti-phospho-H3 (S10) antibody (diluted at 1:1500; #3377, Cell Signaling Technology) in 1% (w/v) BSA in PBS for 1 h at RT and then co-stained for 30 min at 4°C with an Alexa Fluor® 568 goat anti-rabbit secondary antibody (diluted at 1:500; Thermo Fisher Scientific) together with 10 mM DAPI in 1% (w/v) BSA in PBS. For the EdU assay (using the Click-iT® Plus EdU assay, Invitrogen-Thermo Fisher Scientific), untreated or treated CRC-SCs were incubated with 10 µM EdU for 15 h at 37°C, fixed, permeabilized with the Click-iT™ Triton® X-100-based permeabilization reagent and co-stained with the fluorescent dye azide (Click-iT™ reaction cocktail) and DAPI, according to the manufacturer's instructions. For the quantification of the mitochondrial membrane potential, CRC-SCs were stained with tetramethylrhodamine methyl esters (TMRM) as previously described[6, 7]. Cytofluorometric acquisitions were performed by means of a MACSQuant® Analyzer 10 (Miltenyi Biotec, Bergisch Gladbach, Germany) while data were statistically evaluated using the FlowJo software (FlowJo LLC, Ashland, OR). Only the events characterized by normal forward scatter (FSC) and side scatter (SSC) parameters were gated for inclusion in the statistical analysis. Cell

cycle analyses were performed upon exclusion of the sub-G1, while surface marker assessment and TOP-GFP expression were carried out only on viable cells (*i.e.*, those excluding DAPI). Cell death analyses upon shRNA expressing lentiviral transduction were conducted only on the transduced cell population (GFP⁺ cells).

Microsatellite Instability analysis. DNA from patient-matched non-tumoral tissues and CRC-SCs was extracted with the DNeasy mini kit (Qiagen) according to the manufacturers' instruction. MSI analyses were performed using the fluorescent multiplex PCR-based assay (MSI Analysis System kit, Version 1.2, Promega), which is based a fluorescent multiplex PCR reaction for detecting the amplification of five mononucleotide repeat markers (BAT-25, BAT-26, MONO-27, NR-21 and NR-24) [8, 9]. Denatured PCR products were analyzed by capillary electrophoresis in an ABI Prism[®] 3500 Genetic Analyzer using POP-4[®] polymer (both from Applied Biosystems; Thermo Fisher Scientific.), according to manufacturer's instructions (Promega). For the purpose of prognostic evaluation, microsatellite status was determined upon analysis with GeneMapper[®] software, version 4.1 (Applied Biosystems) and MSI status was categorized as follow: MSI, ≥ 1 altered microsatellite markers out of 5; MSS, no altered microsatellite markers)[10, 11].

Microscopy. The immunofluorescence detection of DNA damage markers was performed as previously described[12, 13]. Briefly, dissociated CRC-SC spheroids were fixed in 4% (w/v) paraformaldehyde in PBS and deposited on poly-L-lysine-coated glass slides. Air-dried slides were then permeabilized with 0.1% (v/v) Triton X-100 (Amersham Biosciences; GE Healthcare Life Sciences, Little Chalfont, UK) in PBS for 15 min, incubated in 5% (w/v) BSA in PBS for 30 min and immunostained overnight at 4 °C with antibodies specific for the phosphorylated form of RPA32 (S4/S8) (diluted at 1:250; Bethyl Laboratories) or γ H2AX (S139) (diluted at 1:400; Cell Signaling Technology) followed by incubation with the appropriate Alexa Fluor conjugates (diluted at 1:600; Molecular Probes-Thermo Fisher Scientific). Hoechst 33342 at doses of 10 μ M was used

to counterstain nuclei. Confocal fluorescence images were captured using a FV1000 spectral confocal microscope (Olympus, Tokyo, Japan) equipped with a 40X (N.A. 1.3) and 60X (N.A. 1.35) oil immersion objectives and the Olympus Fluoview software. Signals from different probes were acquired in sequential scan mode to avoid crossover and image analysis was performed with the open source software ImageJ v1.5 (freely available from the National Institute of Health, Bethesda, MD at the address <http://rsb.info.nih.gov/ij/>). For the comet assay, CRC-SCs left untreated or administered with LY2606368 as indicated in Figure legend were resuspended in low-melting-point agarose (0.7% in H₂O; Sigma-Aldrich) and layered on slides previously prepared with normal melting agarose (1% in H₂O, Sigma-Aldrich). Upon immersion for 1 h at 4 C in a lysis solution containing 0.1 M Na₂EDTA, 2.5 M NaCl and 10 mM Tris (pH 10) supplemented with 1% Triton X-100 and 10% DMSO 15 min before performing the experiment, slides underwent electrophoresis at 1.0 V/cm (30 V) and 300 mA for 25 min in a running buffer containing 0.75 g glycine, 0.59 g NaCl in 1L in H₂O (pH 12.9-13.0). Slides were then neutralized for 30 min with 0.3 M sodium acetate in 90% EtOH, dehydrated for 2h with 100% cold EtOH, dried at RT and finally stained with 25 µg/mL PI in PBS. Fluorescence images of comets were captured at 4X and 10X objective magnification using an inverted microscope (Nikon Eclipse TS100F; Nikon, Melville, NY) and analyzed by using CASPLab v1.2.2 software as described in [14]. At least 100 nuclei for per sample condition were scored. The tail moment was automatically calculated by the CASPLab software and is the product of the tail length and the fraction of total DNA in the tail and was used as a proxy measurement of the DNA damage.

Metaphase spreads were performed according to standard protocols[15]. Briefly, CRC-SCs were treated for 5 h with 5 µM colchicine (Sigma-Aldrich) to enrich the fraction of mitotic cells. At the end of the treatment, cells were collected and incubated with 75 mM KCl (J.T.Baker) for 12 min at 37°C prior to fixation in freshly prepared Carnoy solution (3:1 v:v methanol:acetic acid, both from Sigma-Aldrich) and storage at -20°C. Fixed cells were then dropped onto glass slides, air-dried and

mounted with a solution containing the DNA dye DAPI and Prolong-Gold antifade (Molecular Probes-Thermo Fisher Scientific) for cytogenetic analysis. Metaphases were captured using the Axio-Imager M1 microscope equipped with a coupled charged device (CCD) camera (Zeiss, Oberkochen, Germany) and images (100 metaphases for each sample) analyzed with ImageJ v1.5 .

Immunohistochemistry. CRC-SCs-derived xenografts were removed, fixed in formalin overnight at 4°C and paraffin embedded. Tissues were sectioned for subsequent immunohistochemical staining using the following primary antibodies: anti-phospho-ATM (S1981) (diluted at 1:200; #200-301-400, Rockland, Limerick, PA) and phospho-RPA32 (S4/S8) (diluted at 1:100; Bethyl Laboratories) in the Bond-III automated immunostainer (Leica Microsystems GmbH, Wetzlar, Germany). A citrate buffer, pH 6 was used as antigen retrieval according to the manufacturer's protocol. Images were obtained at 40X magnification by using the Eclipse 55i microscope (Nikon) equipped with a suitable software (Eureka Interface System, Menarini, Florence, Italy). The levels of phosphorylation of ATM and RPA32 were evaluated in terms of proportion of expressing tumor cells (from 0% to 100%) and the intensity of staining (0: negative, 1+: weak, 2+: moderate, 3+: strong) and analyzed as categorical variables. The two scores were multiplied (maximum = 300) and the median score of all tumors was used to classify low and high expressing CRC-SCs-derived xenografts.

Statistical procedures. Unless otherwise specified, all experiments were carried out in triplicate parallel instances and independently repeated at least three times, data were analyzed with Microsoft Excel (Microsoft, Redmond, WA), GraphPad Prism (GraphPad Software, San Diego, CA) or "R" software (see above). Statistical significance of data from most *in vitro* and from *in vivo* studies was evaluated by one- or two-way ANOVA and Bonferroni multiple comparisons test (**Figures 1D-1G, 4A-4E, 6A, 6B, 6D, 6E, S2A, S5B, S5C, S5E, S5F, S6B, S7B, S8A, S8B, S9A**). The statistical analysis of RPPA data was performed based on the distribution and nature of the

data. Briefly, due to low sample size for single time and concentration points in each CRC-SC and the presence of non-parametric distributions, as assessed by Lilliefors and Shapiro-Wilks tests, data were assumed to have non-parametric distribution. Thus, Kruskal-Wallis non-parametric test was applied to test the non-random variance of basal, time-pooled protein and phospho-protein expression levels in the three classes of LY2636068 sensitivity. When Kruskal-Wallis test produced a significant variation among the three groups of CRC-SCs, Wilcoxon signed rank test was applied to test the statistical significance of the difference in protein expression levels, between LY2606368-high and -low sensitive CRC-SCs. Due to the intrinsic presence of multiple hypotheses, *P* values were subsequently adjusted using Benjamini & Hochberg's correction (alias 'FDR' or false discovery rate) (box plots in left panels of **Figures 2B, 3A, 3B, 4F, S4A, S10A**). Vice versa, for the analysis of time- and concentration-dependent protein and phospho-protein expression levels among the three groups of LY2606368 sensitivity (*i.e.*, high, medium and low) a factorial ANOVA design (with type-III sums of squares) was used to test the statistical significance of the interaction between the time, concentration and LY2606368 sensitivity in explaining RPPA expression levels. In line with the criteria used for previous RPPA data analyses, Tuckey's honestly significant difference (HSD) test was used to correct for the presence of multiple comparisons (kinetics in right panels of **Figures 2B, 3A, 3B, 4F, S4A, S10A; and Figure S4B-E**). Statistical analysis of COMET assay data were performed by Kruskal-Wallis non-parametric test followed by Wilcoxon signed rank test and *P* value adjustment using Benjamini & Hochberg's correction (false discovery rate, FDR) (**Figure 3D**). The 'R' packages used for the aforementioned RPPA data analyses are the following: 'base', 'plyr', 'dplyr', 'tidyr', 'coin', 'nortest' and 'lsmeans'. Concerning IHC, the Spearman's correlation coefficient was calculated to assess the correlation between ATM phosphorylation and RPA32 phosphorylation. Finally, the Pearson's Chi-squared test, and the Fisher's Exact test, when appropriate, were applied to evaluate the relationship between LY2606368 sensitivity and the phosphorylation of RPA32, ATM, the ploidy status, the MSI status

and the TP53 mutational status (**Figure 3E, 3F, 5E and text**). We considered statistically significant *P* values less than 0.05. Statistical analyses were carried out using SPSS software (SPSS version 21, SPSS Inc., Chicago, IL) (**Figure 3E,F**).

References

- 1 Ricci-Vitiani L, Pallini R, Biffoni M, Todaro M, Invernici G, Cenci T, *et al.* Tumour vascularization via endothelial differentiation of glioblastoma stem-like cells. *Nature* 2010;**468**:824-8.
- 2 Sato T, Vries RG, Snippert HJ, van de Wetering M, Barker N, Stange DE, *et al.* Single Lgr5 stem cells build crypt-villus structures in vitro without a mesenchymal niche. *Nature* 2009;**459**:262-5.
- 3 De Angelis ML, Zeuner A, Policicchio E, Russo G, Bruselles A, Signore M, *et al.* Cancer Stem Cell-Based Models of Colorectal Cancer Reveal Molecular Determinants of Therapy Resistance. *Stem cells translational medicine* 2016;**5**:511-23.
- 4 Vitale I, Senovilla L, Jemaa M, Michaud M, Galluzzi L, Kepp O, *et al.* Multipolar mitosis of tetraploid cells: inhibition by p53 and dependency on Mos. *The EMBO journal* 2010;**29**:1272-84.
- 5 Horst D, Chen J, Morikawa T, Ogino S, Kirchner T, Shivdasani RA. Differential WNT activity in colorectal cancer confers limited tumorigenic potential and is regulated by MAPK signaling. *Cancer Res* 2012;**72**:1547-56.
- 6 Vitale I, Jemaa M, Galluzzi L, Metivier D, Castedo M, Kroemer G. Cytofluorometric assessment of cell cycle progression. *Methods in molecular biology* 2013;**965**:93-120.
- 7 Jemaa M, Vitale I, Kepp O, Berardinelli F, Galluzzi L, Senovilla L, *et al.* Selective killing of p53-deficient cancer cells by SP600125. *EMBO molecular medicine* 2012;**4**:500-14.
- 8 Farahani N, Nikpou P, Emami MH, Hashemzadeh M, Zeinalian M, Shariatpanahi SS, *et al.* Evaluation of MT1XT20 Single Quasi-Monomorphic Mononucleotide Marker for Characterizing Microsatellite Instability in Persian Lynch Syndrome Patients. *Asian Pac J Cancer Prev* 2016;**17**:4259-65.

- 9 Patil DT, Bronner MP, Portier BP, Fraser CR, Plesec TP, Liu X. A five-marker panel in a multiplex PCR accurately detects microsatellite instability-high colorectal tumors without control DNA. *Diagn Mol Pathol* 2012;**21**:127-33.
- 10 Jensen SA, Vainer B, Kruhoffer M, Sorensen JB. Microsatellite instability in colorectal cancer and association with thymidylate synthase and dihydropyrimidine dehydrogenase expression. *BMC Cancer* 2009;**9**:25.
- 11 Loukola A, Eklin K, Laiho P, Salovaara R, Kristo P, Jarvinen H, *et al.* Microsatellite marker analysis in screening for hereditary nonpolyposis colorectal cancer (HNPCC). *Cancer Res* 2001;**61**:4545-9.
- 12 Michels J, Vitale I, Galluzzi L, Adam J, Olaussen KA, Kepp O, *et al.* Cisplatin resistance associated with PARP hyperactivation. *Cancer research* 2013;**73**:2271-80.
- 13 Hoffmann J, Vitale I, Buchmann B, Galluzzi L, Schwede W, Senovilla L, *et al.* Improved cellular pharmacokinetics and pharmacodynamics underlie the wide anticancer activity of sagopilone. *Cancer research* 2008;**68**:5301-8.
- 14 Konca K, Lankoff A, Banasik A, Lisowska H, Kuszewski T, Gozdz S, *et al.* A cross-platform public domain PC image-analysis program for the comet assay. *Mutat Res* 2003;**534**:15-20.
- 15 Boileve A, Senovilla L, Vitale I, Lissa D, Martins I, Metivier D, *et al.* Immunosurveillance against tetraploidization-induced colon tumorigenesis. *Cell cycle* 2013;**12**:473-9.

Legends to Supplementary Figures

Figure S1. Identification of LY2606368 as the most effective DNA damage response (DDR) inhibitor in killing CRC-SCs.

Five CRC-SCs - *i.e.*, #1, #2, #3, #4 and #5 - were left untreated or treated for 72 h with a dose-range of 13 specific pharmacological inhibitors of DDR players (see also **Figure 1B**). Afterwards, cell proliferation and viability were evaluated by CellTiter-Glo[®] assay. Dose-response curves and the corresponding IC₅₀ (μM) and *P* values are reported for all inhibitors tested.

Figure S2. Preferential CSC targeting of LY2606368 in CRC-SCs.

(A) CRC-SCs differing for their LY2606368 (LY) sensitivity were left untreated or exposed to LY2606368 as illustrated, and then co-stained with the vital dye DAPI and an antibody directed against the CRC-SC marker ephrin B2 (EFNB2) prior to cytofluorimetric analysis. Representative plots for one LY2606368-sensitive (#16) and one LY2606368-resistant (#7) CRC-SCs left untreated (control) or treated with 100 nM LY2606368 as well as a histogram reporting quantitative data (means±SEM; n=4) concerning the fold change decrease of EFNB2⁺ cells as compared to control conditions are reported. Numbers in plots indicate the percentages of corresponding events. Note that only viable cells (*i.e.*, those excluding DAPI) were included in the analysis and that at least 2 CRC-SCs from each group of LY2606368 sensitivity were employed. **P*<0.05, ***P*<0.01, ****P*<0.001 (two-way ANOVA and Bonferroni post-hoc tests) as compared to the corresponding untreated CRC-SCs.

(B) Representative LY2606368-sensitive CRC-SCs were transduced with a lentiviral vector containing the WNT-pathway two-color reporter TOP-GFP.mC. Upon infection, CRC-SCs were treated with puromycin followed by FACS-mediated sorting of transduced (those constitutively expressing nuclear mCherry; mCherry⁺) cells. Thereafter, these cells were treated for 48 h with 50 nM LY2606368 as depicted, stained with the vital dye DAPI and analyzed by flow-cytometry for

GFP expression according to the evidence that CSCs are the subpopulation of cells with highest WNT activity (*i.e.*, those highly expressing GFP, GFP^{high+} cells). Only viable cells (*i.e.* those excluding the vital dye DAPI) were included in the analysis. Representative profiles of untreated or LY2606368-treated CRC-SCs (numbers in plots indicate the percentages of GFP^{high+} cells) and a histogram reporting quantitative data (means±SEM; n=3) are shown. * $P < 0.05$, ** $P < 0.01$, *** $P < 0.001$ (one-way ANOVA and Bonferroni post-hoc tests) as compared to the corresponding untreated CRC-SCs.

In all panels, LY2606368-high and -low sensitive CRC-SCs are depicted in red and green, respectively.

Figure S3. Reverse phase protein array (RPPA) analyses on CRC-SCs treated with LY2606368.

Nine representative CRC-SCs, 3 from each group of LY2606368 sensitivity, and the ATCC cell lines HCT 116 and HT-29 were left untreated or treated for 4h with 10, 50 and 100 nM LY2606368 and then subjected to RPPA analysis. The hierarchical clustering of RPPA results obtained on cells untreated (white) or treated with LY2606368 (black) is represented. LY2606368 high, medium and low (also referred to as resistant) sensitive CRC-SCs are depicted in red, yellow and green, respectively. See also **Figure 2A**.

Figure S4. Phosphorylation levels of DDR players and histone H3 in CRC-CSCs upon LY2606368 administration.

Nine representative CRC-SCs, 3 from each group of LY2606368 sensitivity, were left untreated or administered with LY2606368 at low doses (10, 50 and 100 nM) in a time-course experiment of 1 h, 4 h, 9 h and 24 h. Samples were then subjected to reverse phase protein array (RPPA) analysis. The box-plot in panel (A) illustrates the basal levels of phosphorylated ATR (pATR) (S428) in untreated CRC-SCs at all time points analyzed by RPPA pooled for each sensitivity group.

* $P < 0.05$, ** $P < 0.01$, *** $P < 0.001$, Wilcoxon signed-rank test followed by P value adjustment by FDR for the comparison: high vs. low sensitive CRC-SCs. In the right part of (A) and in (B-E), the full time- and dose-dependent RPPA kinetics of phosphorylated ATR (pATR_S428), CHK1 (pCHK1_S317 and pCHK1_S345), CHK2 (pCHK2_T68) histone H3 (pH3_S10) shown as means \pm SD of CRC-SCs grouped by LY2606368 sensitivity are illustrated. * $P < 0.05$, ** $P < 0.01$, *** $P < 0.001$, factorial ANOVA design followed by P value adjustment (Tuckey's HSD) for the comparison: 100 nM LY2606368-treated vs. untreated CRC-SCs of the same sensitivity group. § $P < 0.05$, §§ $P < 0.01$, §§§ $P < 0.001$, factorial ANOVA design followed by P value adjustment (Tuckey's HSD) for the comparison: high vs. low sensitive CRC-SC treated with 100 nM LY2606368. A.U., arbitrary units. See also **Figure 2**.

In all panels, LY2606368-high, -medium and -low sensitive CRC-SCs are depicted in red, yellow and green, respectively.

Figure S5. Phosphorylation levels of ATM and other DDR players in CRC-CSCs at the baseline and upon LY2606368 administration

(A-H). CRC-SCs from each group of LY2606368 sensitivity were left untreated or administered with LY2606368 as indicated, and then subjected to western-blot analyses with antibodies recognizing the phosphorylated or total forms of ATM, CHK2, ATR or CHK1. Nucleolin or β -Actin levels were assessed to monitor equal lane loading. Histograms in (A,D,G,H) report the densitometric analysis of the western blots showed in **Figure 2C**, performed by calculating the relative optical density of phosphorylated or total forms of the indicated protein normalized to nucleolin or β -Actin levels (see **Supplementary information** for more details). Values obtained for the phosphorylated form were then normalized to those of the corresponding total form. Histograms in panels (B) and (E) illustrate levels of phosphorylated ATM normalized to total ATM (pATM/ATM) (B) and levels of phosphorylated ATR normalized to total ATR (pATR/ATR) in

untreated CRC-SCs quantified by densitometry as reported above and then pooled for each sensitivity group. Histograms in panel (C) and (F) represent the increase in the levels of pATM/ATM (C) and pATR/ATR (F) upon LY2606368 exposure quantified by densitometry as reported above and then pooled for each sensitivity group. In the presence of hardly detectable levels, the increase was approximated to 1. The analyses were performed on at least 4 western blots, including the representative ones shown in **Figure 2C**. * $P < 0.05$, ** $P < 0.01$, *** $P < 0.001$ (two-way ANOVA and Bonferroni post-hoc tests) for the comparison: high vs. low sensitive. CRC-SCs. LY2606368-high, -medium and -low sensitive CRC-SCs are depicted in red, yellow and green, respectively.

Figure S6. Phosphorylation levels of RPA32 in CRC-CSCs at the baseline and upon LY2606368 administration.

(A-B) Untreated CRC-SCs from each group of LY2606368 sensitivity were subjected to western-blot analyses with antibodies recognizing the phosphorylated form of RPA32 (pRPA32_S4/S8) and total RPA32. β -Actin levels were assessed to ensure equal lane loading. The histogram in (A) represents the densitometric analysis of the western blots showed in **Figure 3C** for pRPA32_S4/S8. In (B), the quantification of pRPA32_S4/S8 levels normalized to total RPA32 (pRPA32/RPA32) in untreated CRC-SCs pooled for each sensitivity group is reported. The analyses were performed on 2 western blots, including the representative one reported in **Figure 3C**. * $P < 0.05$, ** $P < 0.01$, *** $P < 0.001$ (two-way ANOVA and Bonferroni post-hoc tests) for the comparison: high vs. low sensitive. For more details on the densitometry, normalization to the total form and statistical analysis, refer to legend of **Figure S5** and **Supplementary information**.

(C) Western-blot analyses (6h of treatment with 100 nM LY2606368) performed with antibodies recognizing the phosphorylated form of RPA32 (pRPA32_S4/S8) and total RPA32. β -Actin levels were monitored to ensure equal loading of lanes. One representative western-blot is shown. Note

that the basal level of pRPA32_S4/S8 is hardly detectable due to its huge increase in sensitive CRC-SCs upon LY2606368 administration. Therefore, densitometry of basal levels of RPA32-normalized pRPA32_S4/S8 was performed on further western blot series whose results are reported in **(A) and (B), and Figure 3**.

In all panels, LY2606368-high, -medium and -low sensitive CRC-SCs are depicted in red, yellow and green, respectively.

Figure S7. γ H2AX levels in CRC-SCs.

(A,B) The illustrated CRC-SCs were left untreated (-) or administrated with 100 nM LY2606368 for 6h (+) and then subjected to western-blot analyses with antibodies recognizing γ H2AX or β -Actin, whose levels were monitored to ensure equal loading of lanes. One representative western-blot and the densitometry of the western blots performed as described in **Figure S5** and **Supplementary information** are shown in **(A)**. Note that all CRC-SCs, 2 from each sensitivity class, were the same used in RPPA studies. LY2606368-high, -medium and -low sensitive CRC-SCs are depicted in red, yellow and green, respectively. In **(B)**, the quantification of γ H2AX or β -Actin levels normalized to β -Actin (γ H2AX/ β -Actin) in untreated CRC-SCs pooled for each sensitivity group is reported. The analyses were performed on 4 western blots, including the representative one reported in **(A)**. * P <0.05, ** P <0.01, *** P <0.001 (two-way ANOVA and Bonferroni post-hoc tests) for the comparison: high vs. low sensitive. For more details on the densitometry, normalization to the total form and statistical analysis, refer to legend of **Figure S6** and **Supplementary information**.

Figure S8. Basal levels of endogenous DNA damage in CRC-SCs.

(A,B) A representative number of CRC-SCs differing for their sensitivity to LY2606368 was left untreated and then subjected immunofluorescence staining with antibodies recognizing the phosphorylated form of RPA32 (pRPA32_S4/S8) **(A)** or γ H2AX **(B)**. The DNA intercalating dye

Hoechst was employed to counterstain nuclei. The quantification of the percentage of cells displaying more than 5 foci of pRPA32 or γ -H2AX or a pan-nuclear staining is represented (means \pm SEM, n=2). Results are reported as means \pm SEM. * P <0.05, ** P <0.01, *** P <0.001 (one-way ANOVA and Bonferroni post-hoc tests), as compared to LY2606368-low sensitive CRC-SCs.

LY2606368-high, -medium and -low sensitive CRC-SCs are depicted in red, yellow and green, respectively.

Figure S9. Impact of CHK1 depletion on CRC-SC survival.

(A) CRC-SCs from each class of LY2606368 sensitivity were transfected with an unrelated small interfering (si) RNA (siCTR) or specific pools of siRNAs directed against CHK1 (siCHK1A and siCHK1B). Samples were collected upon 96h and subjected by CellTiter-Glo[®] assay for measuring proliferation/viability (means \pm SEM; n=5; at least 2 CRC-SCs from each group of LY2606368 sensitivity were employed) * P <0.05, ** P <0.01, *** P <0.001 (two-way ANOVA and Bonferroni post-hoc test) as compared siCTR-transfected CRC-SCs.

(B,C) CRC-SCs differing for their LY2606368 sensitivity (at least 2 CRC-SCs from each group of LY2606368 sensitivity) were either transfected with siCTR, siCHK1A and siCHK1B (B) or transduced with lentiviral vectors expressing non-silencing short hairpin (sh) RNA (shCTR) or CHK1-targeting shRNAs (shCHK1A and shCHK1B) (C). Samples were collected and then subjected to western-blot analyses with antibodies recognizing CHK1 or β -Actin, whose levels were monitored to ensure equal loading of lanes. Western-blot for representative CRC-SCs sensitive and resistant to LY2606368 are shown.






In all panels, LY2606368-high and -low sensitive CRC-SCs are depicted in red and green, respectively.

Figure S10. p53 pathway deregulation in CRC-CSCs at the baseline and/or upon LY2606368 administration.

(A) RPPA box-plots (left) of the basal levels of p21 in untreated CRC-SCs pooled for each sensitivity group at all time points, and RPPA time- and dose-response plots (right) of p21 of CRC-SCs grouped by LY2606368 sensitivity. Results are shown as means \pm SD. For more insights on RPPA data statistical analysis, refer to legend of **Figure 2B**.

(B) The illustrated CRC-SCs were left untreated or treated with 100 nM LY2606368 (LY) as reported before immunodetection of p21 (by western-blot. β -tubulin levels were used as loading controls. One representative western-blot and the densitometry of the western blots (performed as described in **Figure S5** and **Supplementary information**) are shown.

In all panels, LY2606368-high, -medium and -low sensitive CRC-SCs are depicted in red, yellow and green, respectively.

-  #3 (*KRAS* mutated, *TP53* mutated)
-  #4 (*KRAS* WT, *TP53* mutated)
-  #1 (*KRAS* WT, *TP53* mutated)
-  #2 (*KRAS* mutated, *TP53* mutated)
-  #5 (*KRAS* WT, *TP53* WT)

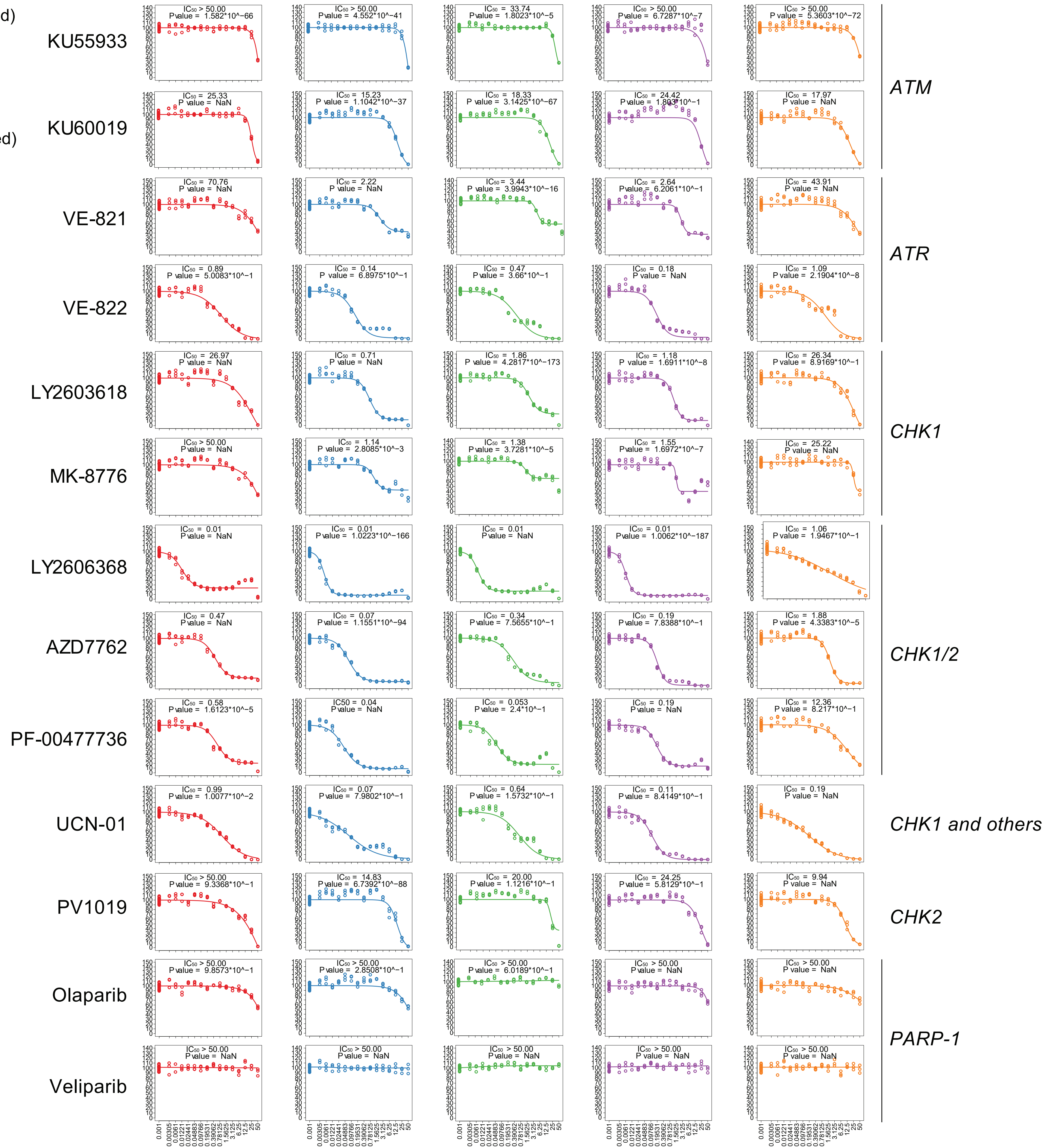
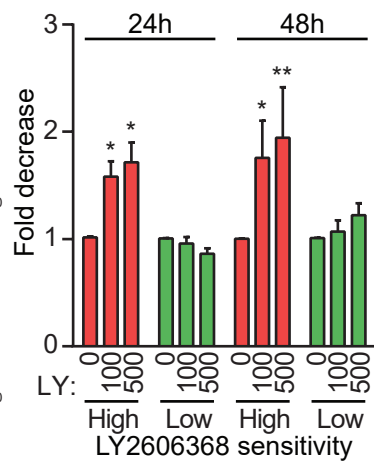
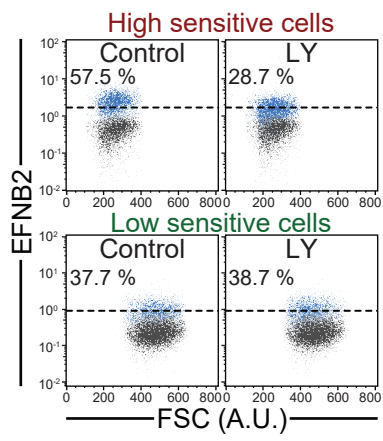
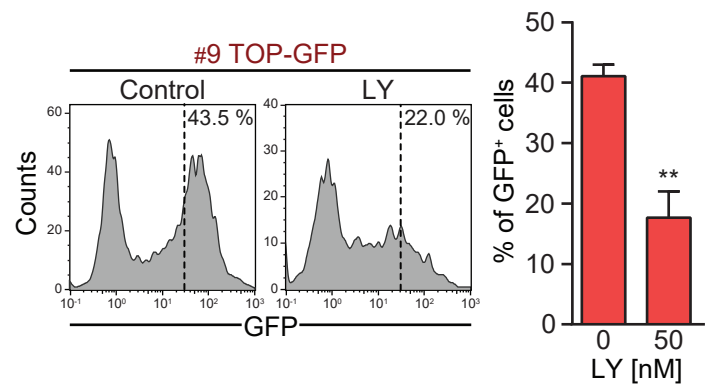


FIGURE S1

A**B****Figure S2**

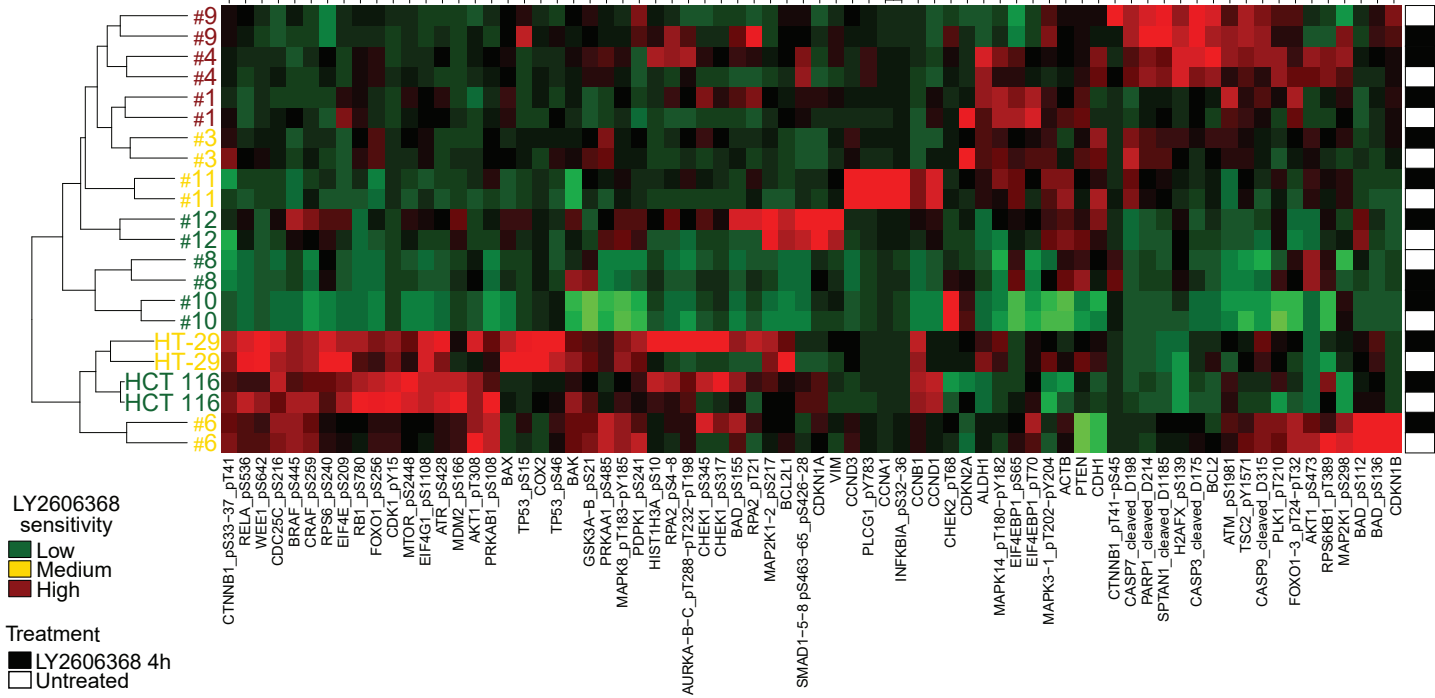
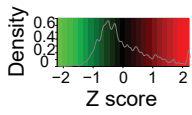


Figure S3

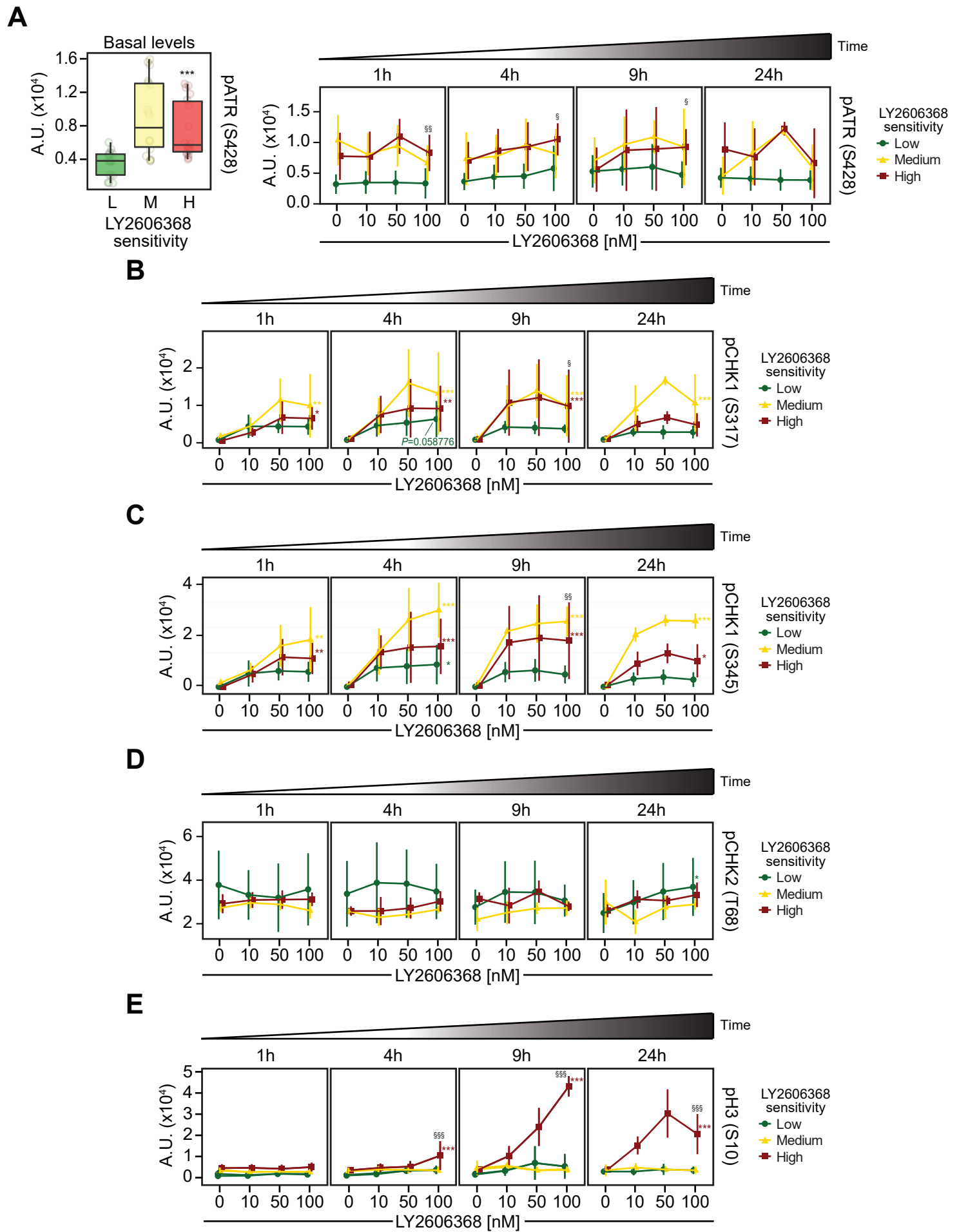


Figure S4

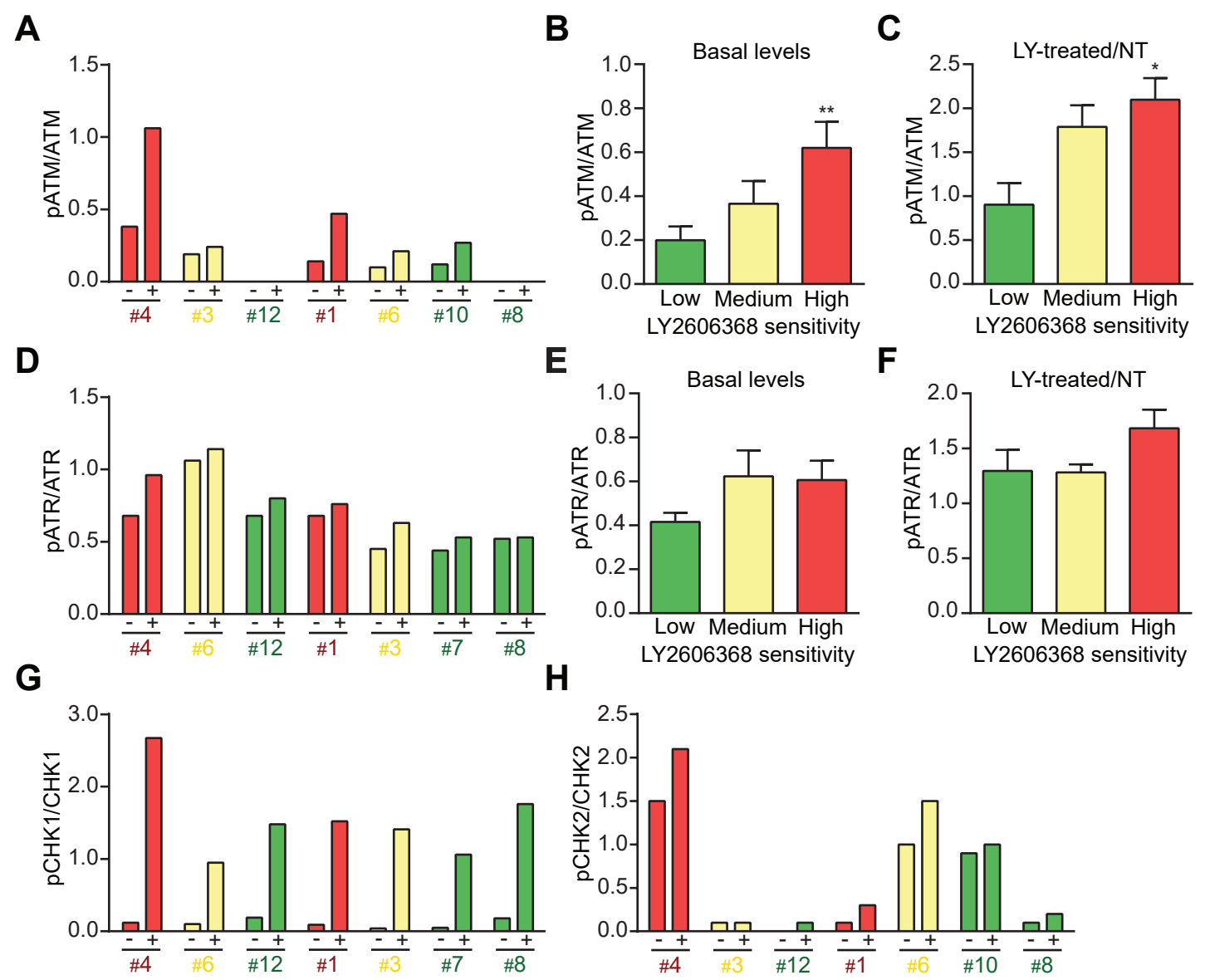


Figure S5

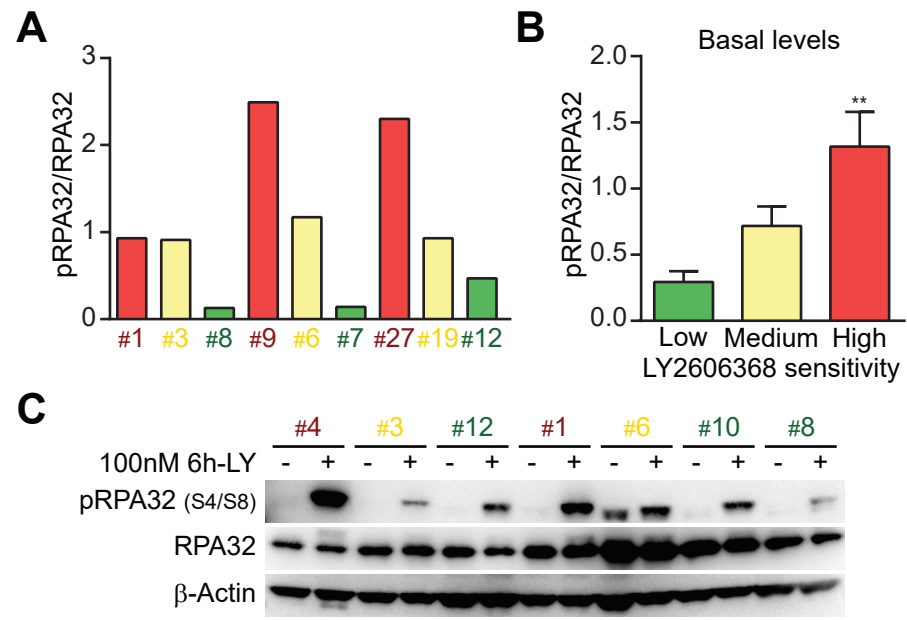


Figure S6

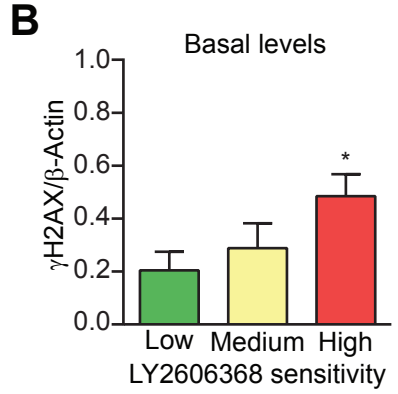
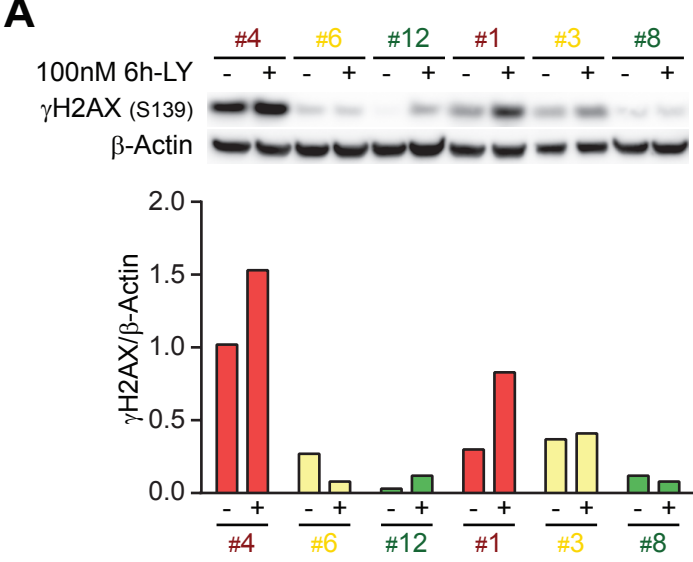
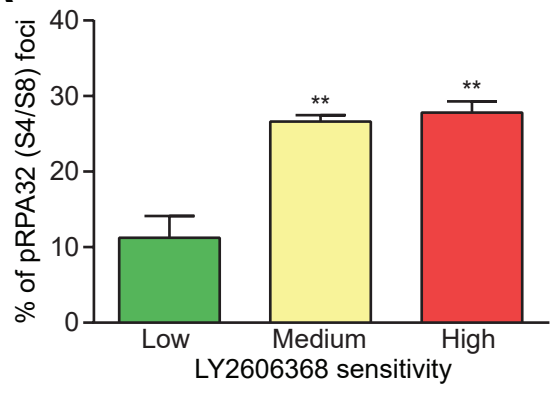
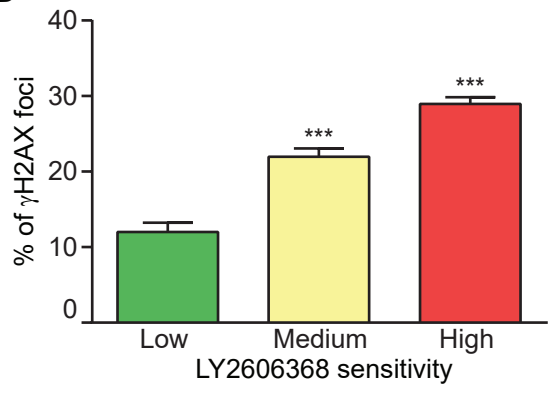


Figure S7

A**B****Figure S8**

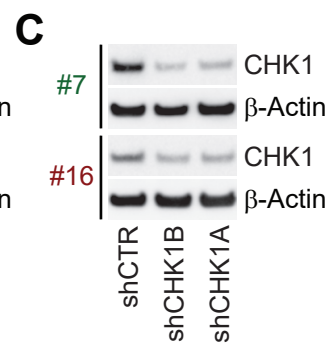
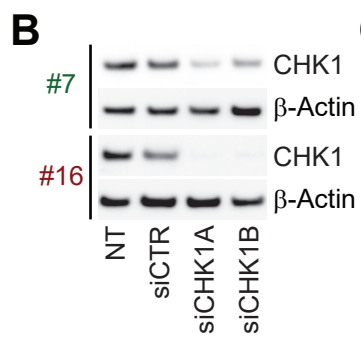
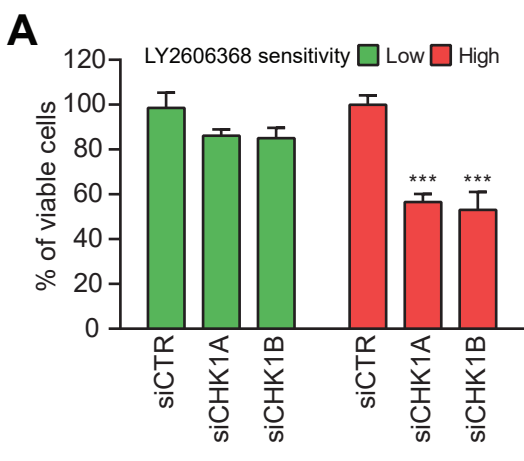
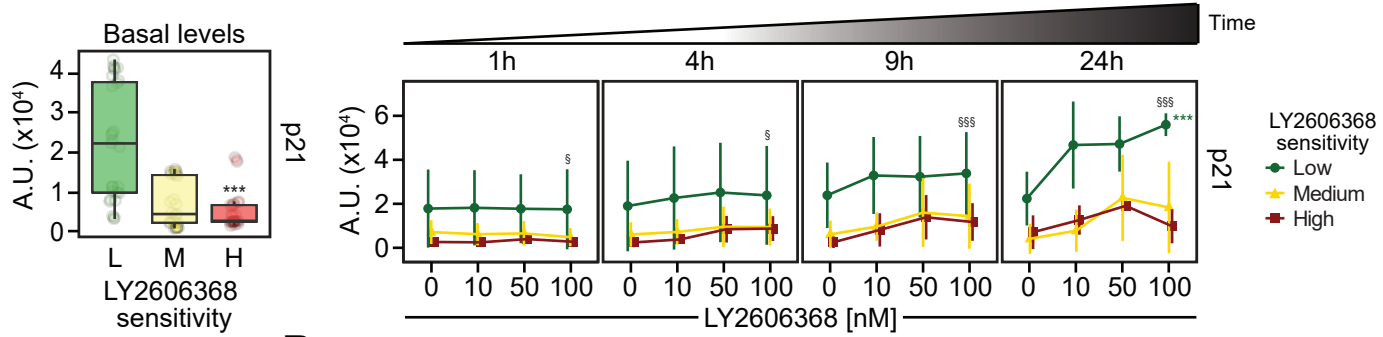
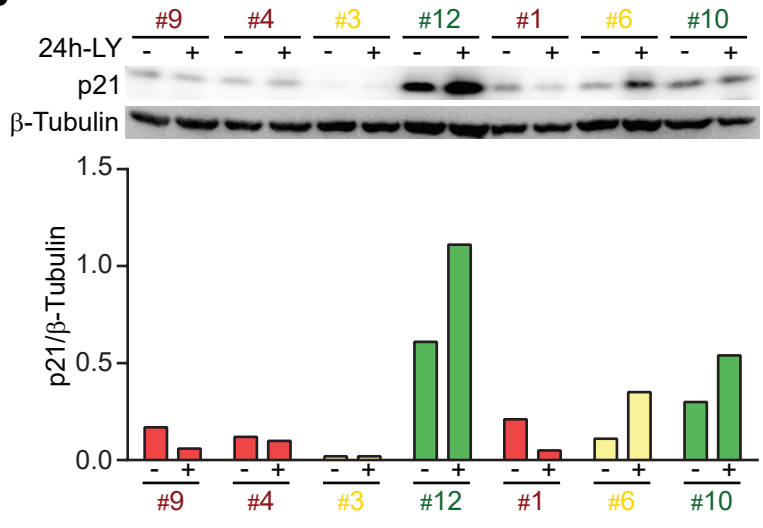


Figure S9

A**B****Figure S10**